Tuberatolides, Potent FXR Antagonists from the Korean Marine Tunicate Botryllus tuberatus

ARTICLE *in* JOURNAL OF NATURAL PRODUCTS · DECEMBER 2010

Impact Factor: 3.8 · DOI: 10.1021/np100489u · Source: PubMed

9 AUTHORS, INCLUDING:

Hyukjae Choi
Yeungnam University
50 PUBLICATIONS **401** CITATIONS

SEE PROFILE

Jungwook Chin
Daegu Gyeongbuk Medical Innovation Fou…
27 PUBLICATIONS **196** CITATIONS

SEE PROFILE

Tuberatolides, Potent FXR Antagonists from the Korean Marine Tunicate *Botryllus tuberatus*

Hyukjae Choi,[†,‡] Hoosang Hwang,[†,‡] Jungwook Chin,[†] Euno Kim,[†] Jaehwan Lee,[†] Sang-Jip Nam,[†] Byoung Chan Lee,[†] Boon Jo Rho,[§] and Heonjoong Kang*[,†,⊥]

Center for Marine Natural Products and Drug Discovery, School of Earth and Environmental Sciences, Seoul National University, NS-80, 151-747, Seoul, Korea

Received July 19, 2010

One isoprenoid, tuberatolide A (**1**), meroterpenoids tuberatolide B (**2**) and 2′-*epi*-tuberatolide B (**3**), and the known meroterpenoids yezoquinolide (**4**), (*R*)-sargachromenol (**5**), and (*S*)-sargachromenol (**6**) were isolated from the Korean marine tunicate *Botryllus tuberatus*. The structures of these compounds were elucidated by NMR, MS, and CD spectroscopic analyses. These terpenoids antagonized the chenodeoxycholic acid (CDCA)-activated human farnesoid X receptor (hFXR) in a cell-based co-transfection assay with IC_{50} values as low as 1.5 μM without significant effect on steroid receptors. Furthermore, they released the co-activator peptide from the CDCA-bound hFXR ligand binding domain in cell-free surface plasmon resonance experiments.

Farnesoid X receptor (FXR) is a ligand-dependent transcription factor in the nuclear receptor superfamily that is highly expressed in the liver and intestine.[1,2] FXR is a bile acid (BA) sensor and plays an important role in cholesterol homeostasis in the human body.[2,3] In recent studies, FXR has been reported to be a promising drug target in the treatment of atherosclerosis. Ligand-activated FXR prevents the progression of atherosclerotic lesion formation in low-density lipoprotein receptor knockout ($LDLR^{-/-}$) and apolipoprotein E knockout ($apoE^{-/-}$) mice.[4] FXR agonists decrease plasma triglyceride levels and increase the synthesis of high-density lipoprotein (HDL) cholesterol by regulating the expression of phospholipid transfer proteins and apolipoproteins such as apolipoprotein C-I (ApoC-I) and apolipoprotein C-IV (ApoC-IV).[5] However, male FXR/LDLR double-knockout mice show a reduced development of atherosclerosis due to the suppressed expression of low-density lipoprotein (LDL) scavenger receptors in macrophages and decreased LDL and cholesterol levels in plasma.[6] Also, atherosclerosis is greatly decreased in female FXR/ApoE double-null mice in spite of increased levels of serum cholesterols and triglycerides.[7] Thus, the therapeutic effect of FXR in atherosclerosis is controversial, and the development of a FXR-specific antagonist is needed to resolve this issue. Since BAs were first reported as the ligands of FXR, many natural and synthetic FXR ligands have been developed.[8−10] Most of the previously reported FXR antagonists have a steroid skeleton.[8,9] The well-known steroidal FXR antagonists guggulsterones also regulate steroid receptors and are unsuitable as chemical tools for studying FXR physiology.[8] Therefore the discovery of nonsteroidal FXR antagonists is desirable.

As part of our continuing investigation of FXR antagonists from marine organisms, the isoprenoid tuberatolide A (**1**) and a pair of diastereomeric meroterpenoids, tuberatolide B (**2**) and 2′-*epi*-tuberatolide B (**3**), were isolated from the Korean marine tunicate *Botryllus tuberatus*, along with known meroterpenoids (**4**−**6**). Herein, we have described the isolation and structure elucidation of **1**−**3**, as well as the characterization of their potent FXR antagonistic effects.

The marine tunicate *B. tuberatus,* collected by scuba, was extracted by a mixed organic solvent, and the resulting extract was fractionated into four fractions based on polarity. The EtOAc-soluble layer, which showed potent FXR antagonism in a cell-based co-transfection assay, was subjected to LH-20 open column chromatography followed by silica flash chromatography. Further bioactivity-guided purification by RP HPLC followed by an enantioselective HPLC gave three novel compounds, tuberatolides A (**1**, 2.0 mg) and B (**2**, 10.5 mg) and 2′-*epi*-tuberatolide B (**3**, 10 mg), in addition to yezoquinolide (**4**, 40 mg), (*R*)-sargachromenol (**5**, 10 mg), and (*S*)-sargachromenol (**6**, 10.5 mg).[11]

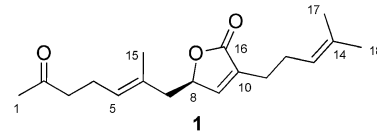

1

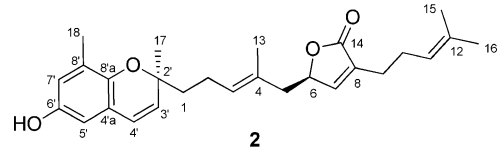

2

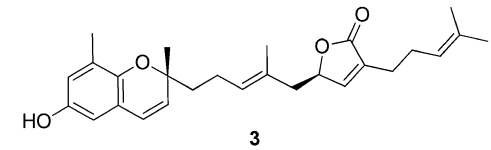

3

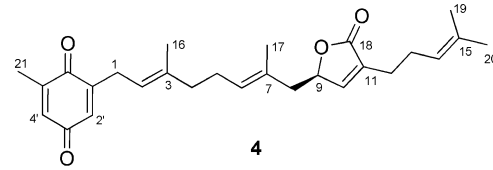

4

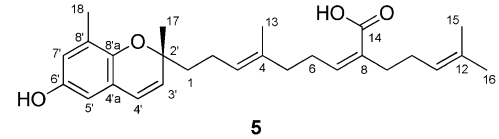

5

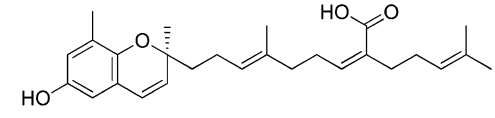

6

The molecular formula of tuberatolide A (**1**) was deduced as $C_{18}H_{26}O_3$ on the basis of the molecular ion peak at *m*/*z* 291.1958

* To whom correspondence should be addressed. Tel: (82)-2-880-5730. Fax: (82)-2-883-9289. E-mail: hjkang@snu.ac.kr.
† Seoul National University.
§ Ewha Womans University.
‡ These two authors contributed equally to the work.
⊥ Also affiliated with RIO/SNU.

10.1021/np100489u
Published on Web 12/13/2010

Table 1. NMR Spectroscopic Data ($CDCl_3$) for Tuberatolides A and B and 2′-*epi*-Tuberatolide B (**1**−**3**)

	1[a]				**2**[b]				**3**[b]	
position	δ_C, mult	δ_H (*J* in Hz)	COSY	HMBC[c]	δ_C, mult	δ_H (*J* in Hz)	COSY	HMBC[c]	δ_C	δ_H
1	30.2, CH_3	2.14, s		13, 1′	40.37, CH_2	1.66, m	12	11, 12, 1′, 10′	40.36	1.67
2	208.5, C				22.75, CH_2	2.17, m	11, 13	11, 13, 1′	22.72	2.17
3	43.5, CH_2	2.49, t (7.5)	12	11, 12, 1′	128.83, CH	5.24, t (7.1)	12, 16	9, 12, 13, 16	128.81	5.24
4	22.6, CH_2	2.30, m	11, 13	10, 1′	129.37, C				129.38	
5	127.6, CH	5.21, t (6.8)	12, 16	9, 13, 16	43.42, CH_2	2.36, m	8	7, 8, 10, 11, 16	43.43	2.37
						2.22, m				2.23
6	130.8, C				80.14, CH	4.96, dt (1.3, 6.9)	7, 9	6, 7, 9	80.11	4.96
7	43.7, CH_2	2.36, m	8	7, 8, 10, 11	148.36, CH	6.98, d (1.3)	5, 8	5, 8, 15	148.33	6.98
		2.26, m								
8	80.5, CH	4.95, dt (1.4, 6.8)	7, 9	7, 9	133.77, C				133.77	
9	148.2, CH	6.98, d (1.4)	8	6, 8, 15	25.28, CH_2	2.30, t (7.0)	4, 7	3, 4, 6, 7, 15	25.29	2.30
10	134.3, C				25.72, CH_2	2.25, m	3, 5	2, 3, 5, 6	25.72	2.24
11	25.6, CH_2	2.32, m	4	3, 4, 6, 7, 15	122.74, CH	5.07, t (6.9)	1, 4, 14	1, 4, 14	122.75	5.07
12	26.1, CH_2	2.25, m	3, 5	2, 3	132.95, C				132.95	
13	123.1, CH	5.05, t (6.9)	4	1, 2, 4, 14	16.57, CH_3	1.65, s		9, 10, 11	16.57	1.65
14	133.1, C				174.05, C				174.03	
15	17.0, CH_3	1.70, s		10, 11	17.80, CH_3	1.60, s	3	1, 2, 3	17.80	1.60
16	174.2, C				25.68, CH_3	1.68, s	3	2, 3	25.69	1.68
17	18.0, CH_3	1.61, s		1, 2, 3	25.89, CH_3	1.36, s	11	13, 1′, 2′	25.86	1.36
18	25.9, CH_3	1.69, s		2, 3, 14	15.52, CH_3	2.13, s		7′, 8′, 9′	15.52	2.14
2′					77.62, C				77.63	
3′					130.40, CH	5.57, d (9.8)	3′	13, 1′, 4′, 10′	130.46	5.57
4′					123.03, CH	6.27, d (9.8)	2′	1′, 4′, 5′, 9′	122.99	6.27
4′a					121.17, C				121.18	
5′					110.23, CH	6.35, d (2.6)	7′	3′, 6′, 9′	110.21	6.34
6′					148.66, C				148.60	
7′					117.01, CH	6.50, d (2.6)	5′	5′, 6′, 9′, 11′	117.00	6.49
8′					126.25, C				126.27	
8′a					144.59, C				144.64	

[a] Measured at 500 MHz for ^1H NMR and 125 MHz for ^{13}C NMR. [b] Measured at 600 MHz for ^1H NMR and 150 MHz for ^{13}C NMR. [c] HMBC correlations, optimized for 8 Hz, are from proton(s) associated with the indicated carbon.

$[M + H]^+$ in the HRFABMS spectrum and the ^{13}C NMR spectrum. Thus, **1** has six degrees of unsaturation. The IR spectrum of **1** showed characteristic absorption bands at 1755 and 1716 cm^{-1}, indicating the presence of an α,β-unsaturated γ-lactone and a ketone, respectively. The ^{13}C NMR spectrum of **1**, in conjunction with DEPT experiments, revealed four methyls, five methylenes, four methines (three olefinic and one bearing oxygen), and five quaternary carbons. Three spin systems, H_2-3/H_2-4/H-5, H_2-7/H-8/H-9, and H_2-11/H_2-12/H-13, were established on the basis of COSY correlations, and the relative positions of these three partial structures were assigned using HMBC correlations from three olefinic methine protons to the adjacent methyl, methylene, and quaternary carbons. The position of the ketone was inferred from HMBC correlations that associated H_3-1 with C-2 and C-3, and H_2-3 and H_2-4 with C-2. The position of the γ-lactone was assigned using the HMBC correlations from H-9 and H_2-11 to C-16 and further supported by the chemical shift of the oxygen-bearing H-8/C-8 (δ_H 4.95/δ_C 80.5). The geometry of C-5/C-6 was assigned as *E* on the basis of the NOESY correlations of H_2-4/H_3-15 and H-5/H_2-7. Thus, it was revealed that **1** is an isoprenoid with a γ-lactone and a methyl ketone group. Complete assignment of the NMR data is given in Table 1.

The molecular formula of tuberatolide B (**2**) was deduced as $C_{27}H_{34}O_4$ on the basis of the molecular ion peak at *m/z* 422.2454 $[M]^+$ in the HREIMS spectrum and the ^{13}C NMR data. The molecular formula of **2** indicated 11 degrees of unsaturation. The IR spectrum of **2** showed characteristic absorption bands at 3370 and 1754 cm^{-1}, indicating the presence of a hydroxy moiety and an α,β-unsaturated γ-lactone moiety, respectively. The ^{13}C NMR spectrum of **2** in conjunction with DEPT experiments revealed five methyls, five methylenes, eight methines (seven olefinic and one bearing an oxygen), and nine quaternary carbons. The ^1H and ^{13}C NMR spectra of **2** were similar to those of **1** with the exception that the methyl ketone group was not observed in **2**. Additionally, two pairs of coupled protons (H-3′/H-4′ and H-5′/H-7′), two singlet methyl protons (H_3-17 and H_3-18), and five quaternary carbons (C-2′, C-4′a, C-6′, C-8′, and C-8′a) were observed in **2**. The HMBC spectrum of **2** showed correlations from H_3-17 to C-1, C-2′, and C-3′; from H_3-18 to C-7′, C-8′, and C-8′a; from H-4′ to C-2′, C-4′a, C-5′, and C-8′a; and from H-5′ to C-4′, C-6′, and C-8′a, suggesting the presence of a chromene group in place of the methyl ketone group of **1**. Therefore, it was revealed that **2** is a meroterpenoid that contains chromene and γ-lactone groups. Complete assignment of the NMR data is given in Table 1.

2′-*epi*-Tuberatolide B (**3**) eluted in a single peak with tuberatolide B (**2**) on RP HPLC. The LREIMS spectrum for **3** was the same as that for **2**, and their NMR spectra were nearly identical except for slight chemical shift differences at C-3′, C-4′, C-6′, and C-8′a in the ^{13}C NMR spectra. Ultimately, **3** was purified from **2** by an enantioselective HPLC (see Supporting Information S7).

Together with **1**−**3**, three previously reported meroterpenoids, yezoquinolide (**4**), (*R*)-sargachromenol (**5**), and (*S*)-sargachromenol (**6**), were also isolated.[11]

The absolute configurations at the C-8 position in tuberatolide A (**1**) and the C-9 position in yezoquinolide (**4**) were determined to be *R* on the basis of negative Cotton effects of the $\pi-\pi^*$ transition, which were observed at 220 and 219 nm, respectively (Figure 1).[12] The absolute configuration of the C-2′ position in (*R*)-sargachromenol (**5**) was also determined to be *R* because the configuration of C-2′ induces negative exciton coupling.[13] The CD spectrum of (*S*)-sargachromenol (**6**) was found to be inverted relative to that of **5**; therefore, the absolute configuration of the C-2′ position in **6** was determined to be *S*.[13] In the enantioselective HPLC chromatograms, the peak areas of tuberatolide B (**2**) and 2′-*epi*-tuberatolide B (**3**) were nearly equal. A CD spectrum of a mixed sample containing **2** and **3** before chiral separation showed negative Cotton effects at 218 nm, which is similar to those of **1** and **4**; therefore, the absolute configuration of C-6 in **2** and **3** was also determined to be *R*. Finally, when compared to those of **5** and **6**, CD measurements of **2** and **3** after the chiral separation showed that the absolute configurations at the C-2′ positions were *S* and *R*, respectively.[13]

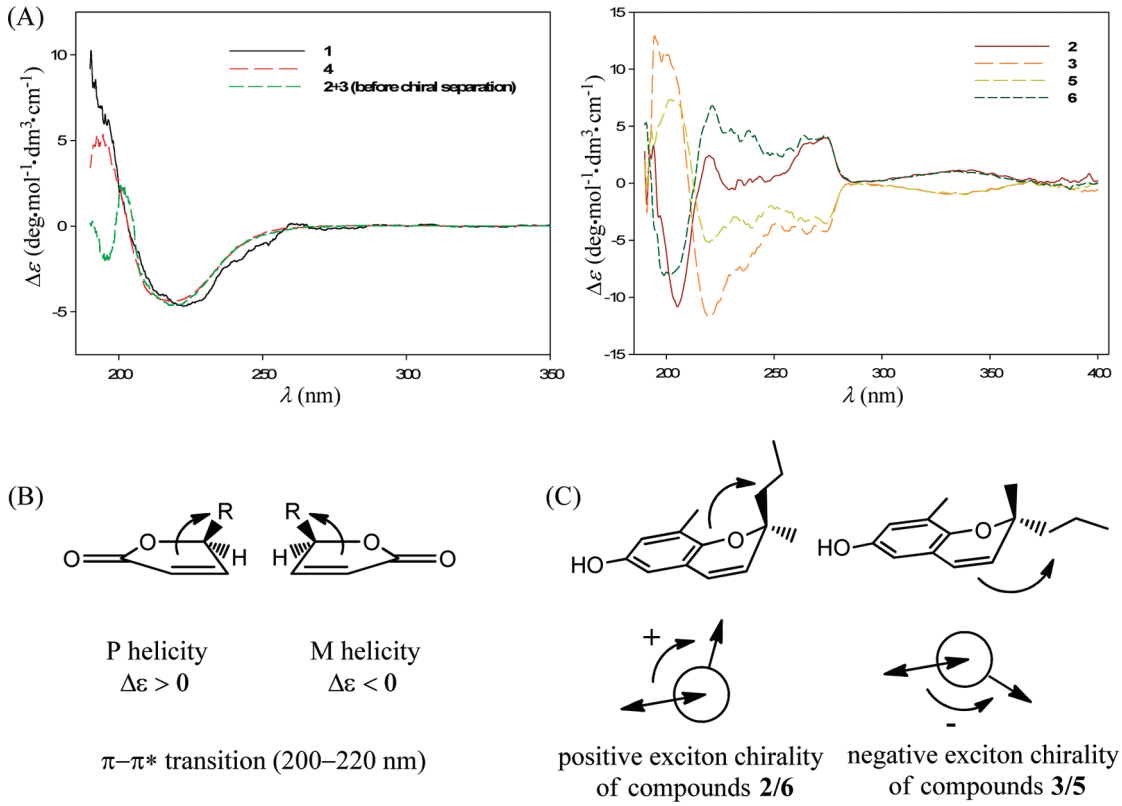

Figure 1. CD spectra of **1**−**6** in MeOH (A), correlation of the butenolide Cotton effects with absolute configuration (B), and exciton coupling on CD spectroscopy associated with the absolute configuration at C-2′ of chromene (C).

The structure of **4**, which contains a 1,4-quinone group, together with the co-isolation of an equivalent amount of **2** and **3** that have diasteromeric chromenes, suggests that **2** and **3** may have originated from **4** not by enzyme-guided biosynthesis but as isolation artifacts by a thermal electrocyclic reaction in which a highly conjugated (and, thus, energetically favorable) keto−enol form of **4** participates as the reaction intermediate (see Supporting Information S17).[14]

Yezoquinolide and sargachromenol were originally reported to be from marine brown algae such as *Sargassum sagamianum* var. *yezoense* and *Sargassum serratifolium*.[11] However, tuberatolides yezoquinolide and sargachromenol have now also been found in the Korean marine tunicate *Botryllus tuberatus*. Therefore, it is possible that these terpenoids are synthesized by symbiotic marine microorganisms in brown algae and tunicates. Alternatively, it is also possible that the source organisms may have similar biosynthetic genes that dictate the biosynthesis of yezoquinolide and sargaquinoic acid, the precursor of sargachromenol.

In a cell-based co-transfection assay, **1**−**6** showed potent inhibition of hFXR transactivation without significant cytotoxicity (Table 2) and without activation of steroid receptors in the transactivation experiments (see Supporting Information S18). In cell-free surface plasmon resonance (SPR) experiments using a BIAcore system, **1**−**6** also decreased the binding affinity of the co-activator peptide SRC-1 to hFXR LBD (Figure 2). It was thus revealed that **1**−**6** are nonsteroidal FXR antagonists. In particular, tuberatolide A (**1**) antagonized chenodeoxycholic acid (CDCA)-dependent hFXR activation in both bioassay systems at low concentrations without any cytotoxicity.

Structurally, **1**−**6** differ from farnesol (a weak agonist of mouse FXR)[15] by the presence of γ-lactones or carboxylic acids at the C-15 position, suggesting that the carbonyl group at C-15 may enhance the hFXR antagonistic effects of **1**−**6**. Despite the possibility that **2**, **3**, **5**, and **6** may be artifacts, they directly bind to hFXR and strongly inhibit its transactivation. Thus, **1**−**6** may help to unravel the controversial function of FXR in atherosclerosis.

Table 2. Inhibition of hFXR Transactivation and Cytotoxicity of **1**−**6**

	IC_{50}, μM[a]	
compound	inhibition of hFXR transactivation	cytotoxicity to CV-1 cell line[b]
1	3.9	>100
2	1.5	31
3	2.5	30
4	5.9	50
5	9.0	45
6	17	56
(*E*)-guggulsterone	44	not determined

[a] Each experiment was repeated more than three times. [b] Cytotoxicity was measured using the MTT method.

Experimental Section

General Experimental Procedures. Optical rotations were measured in MeOH using a 1.0 cm cell on a Rudolph Research Autopol III, #A7214. UV spectra were also recorded in MeOH on a Scinco UVS-2100. CD spectra were taken in MeOH using a JASCO J-715. IR spectra were recorded on KBr plates with a Thermo Nicolet 570. All NMR spectra were recorded on a Bruker Avance DPX-500 or DPX-600 spectrometer using $CDCl_3$ as the solvent. Mass spectrometric data were obtained on JEOL JMS-AX505WA and JMS-600W instruments.

Animal Material. A species of brown encrusting marine tunicate was collected by scuba near Tong-Yong City in the South Sea of Korea. The sample for extraction was frozen immediately after collection. Voucher specimens (CMDD20080028) were anesthetized with 5% menthol in sterilized seawater for 2 h and stored in 10% formalin in sterilized seawater. The animal was taxonomically identified by Dr. B. J. Rho from Ewha Womans University. The voucher was deposited at the Ewha Womans University Natural History Museum in Korea and at the Center for Marine Natural Products and Drug Discovery, Seoul National University, Korea. The tunicate was identified as *Botryllus tuberatus*.

Extraction and Isolation. The frozen animal (1.2 kg, wet wt.) was lyophilized, and the dried specimen (0.4 kg) was extracted thrice with 50% MeOH in DCM. The extracts (18 g) were dried under vacuum.

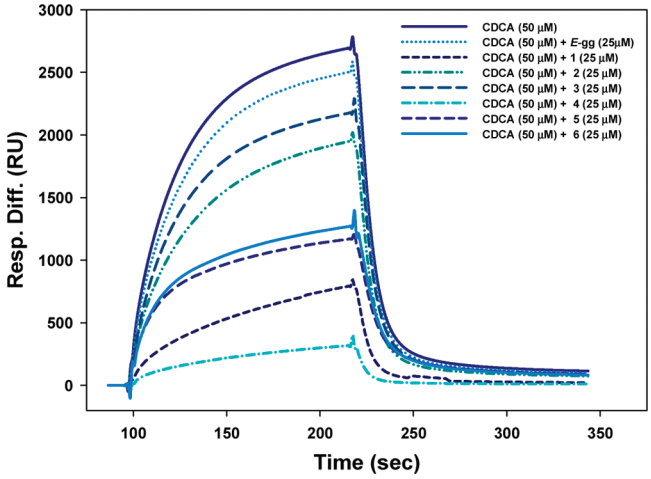

Figure 2. Direct inhibition of the CDCA-induced recruitment of the coactivator peptide to hFXR by compounds **1**−**6**.

The dried residues were dissolved in MeOH and then washed three times with hexanes. After removal of the solvent, the MeOH-soluble fraction (16.5 g) was resuspended in H_2O and partitioned three times with EtOAc. The EtOAc-soluble fraction (1.5 g) inhibited FXR transactivation by over 90% at a concentration of 100 μg/mL. The EtOAc-soluble fraction was further separated into 28 fractions by LH-20 open column chromatography using 100% MeOH. The fractions that displayed activity (over 95% inhibition at 50 μg/mL) against FXR were combined and further fractionated by silica flash chromatography using a stepped gradient elution of hexanes and EtOAc. The fractions eluting with 20−40% EtOAc in MeOH showed potent activity (over 99% inhibition at 50 μg/mL) against FXR, and they were further separated using RP HPLC (Phenomenex PolarRP, 250 × 10 mm, 4 μm, 80 Å, UV = 210 nm), using a mobile phase of 60% CH_3CN in H_2O, to afford tuberatolide A (**1**, 2.0 mg, 1.7×10^{-4}%), yezoquinolide (**4**, 40 mg, 3.3×10^{-3}%), and mixtures of **2/3** (21 mg) and **5/6** (22 mg) as yellow oils. The mixtures were subjected to an enantioselective HPLC (Chiralpak AD-H, 250 × 10 mm, 5 μm, 100 Å, UV = 210 nm). They were then eluted with 75% *n*-hexane in 2-propanol. Four pure compounds, namely, tuberatolide B (**2**, 10.5 mg, 8.8×10^{-4}%), 2′-*epi*-tuberatolide B (**3**, 10 mg, 8.3×10^{-4}%), (*R*)-sargachromenol (**5**, 10 mg, 8.3×10^{-4}%), and (*S*)-sargachromenol (**6**, 10.5 mg, 8.8×10^{-4}%), were finally obtained.

Tuberatolide A (1): yellow oil; $[\alpha]^{25}_D$ −10 (*c* 0.1, $CHCl_3$); UV (MeOH) λ_{max} (log ε) 216 (2.91) nm; CD (*c* 2.4×10^{-4} M, MeOH) λ_{max} ($\Delta\varepsilon$), 220 nm (−4.68); IR (KBr) ν_{max} 2922, 1755, 1716 cm^{-1}; ^1H, ^{13}C, and 2D NMR data, Table 1; LRFABMS *m*/*z* 291 $[M + H]^+$; HRFABMS *m*/*z* 291.1958 $[M + H]^+$ (calcd for $C_{18}H_{27}O_3$, 291.1960).

Tuberatolide B (2): yellow oil; $[\alpha]^{25}_D$ +43 (*c* 1.0, $CHCl_3$); UV (MeOH) λ_{max} (log ε) 209 (3.10), 212 (3.12), 278 (2.57), 310 (2.50) nm; CD (*c* 3.4×10^{-4} M, MeOH) λ_{max} ($\Delta\varepsilon$), 205 nm (−10.81), 220 (2.43), 267 (3.55), 273 (4.00), 335 (1.12); IR (KBr) ν_{max} 3370, 2922, 1754, 1733, 1464, 1203 cm^{-1}; ^1H, ^{13}C, and 2D NMR data, Table 1; LREIMS *m*/*z* 422 $[M]^+$; HREIMS 422.2454 $[M]^+$ (calcd for $C_{27}H_{34}O_4$, 422.2457).

2′-*epi*-Tuberatolide B (3): yellow oil; $[\alpha]^{25}_D$ −76 (*c* 1.0, $CHCl_3$); UV (MeOH) λ_{max} (log ε) 209 (3.10), 212 (3.12), 278 (2.57), 310 (2.50) nm; CD (*c* 3.4×10^{-4} M, MeOH) λ_{max} ($\Delta\varepsilon$), 195 nm (12.73), 220 (−11.82), 265 (−4.48), 274 (−4.25), 339 (−0.98); IR (KBr) ν_{max} 3370, 2922, 1754, 1733, 1464, 1203 cm^{-1}; ^1H, ^{13}C, and 2D NMR data, Table 1; LREIMS *m*/*z* 422 $[M]^+$; HREIMS 422.2453 $[M]^+$ (calcd for $C_{27}H_{34}O_4$, 422.2457).

Yezoquinolide (4): yellow oil; $[\alpha]^{25}_D$ −22 (*c* 1.0, $CHCl_3$); CD (*c* 3.4×10^{-4} M, MeOH) λ_{max} ($\Delta\varepsilon$), 219 nm (−4.39).

(*R*)-Sargachromenol (5): yellow oil; $[\alpha]^{25}_D$ −68 (*c* 1.0, $CHCl_3$); CD (*c* 3.4×10^{-4} M, MeOH) λ_{max} ($\Delta\varepsilon$), 199 nm (−8.08), 221 (6.78), 264 (4.19), 2.74 (4.16), 334 (1.05); ^1H, ^{13}C, and 2D NMR data, see Supporting Information; HREIMS 424.2612 $[M]^+$ (calcd for $C_{27}H_{36}O_4$, 424.2613).

(*S*)-Sargachromenol (6): yellow oil; $[\alpha]^{25}_D$ +88 (*c* 1.0, $CHCl_3$); CD (*c* 3.4×10^{-4} M, MeOH) λ_{max} ($\Delta\varepsilon$), 202 nm (7.34), 220 (−5.18), 264 (−3.35), 274 (−3.49), 338 (−0.97); ^1H, ^{13}C, and 2D NMR data, see Supporting Information; HREIMS 424.2609 $[M]^+$ (calcd for $C_{27}H_{36}O_4$, 424.2613).

Cell-Based Co-transfection Assay. CV-1 cells were seeded in 96-well plates with Dulbecco's modified Eagle's medium (GIBCO) supplemented with 10% resin-charcoal-stripped fetal bovine serum and then incubated in humidified air containing 5% CO_2 at 37 °C for 24 h. Transient co-transfection with pCMX-hFXR, CMX β-GAL, and Tk-$(EcRE)_6$-LUC was carried out using SuperFect (Qiagen), according to the manufacturer's instructions. After incubation for 24 h, co-transfected cells were treated with either a control vehicle (DMSO) or the indicated compounds for hFXR agonist testing. The ligands were co-treated with 50 μM chenodeoxycholic acid (CDCA) to test for hFXR antagonist activity. Cells were harvested at 24 h, and luciferase activities were assayed as described previously.[1] Luciferase activities were normalized to the β-galactosidase activity expressed from the control plasmid CMX-β-GAL. Each transfection was performed in triplicate.

Surface Plasmon Resonance (SPR) Spectroscopy. Direct binding of **1**−**6** to the ligand binding domain (LBD) of hFXR was monitored by SPR spectroscopy using a BIAcore system.[16] hFXR LBD (4 μM) was preincubated for 1 h with either (*E*)-guggulsterone or **1**−**6** in the presence of 50 μM CDCA and was injected over the sensor chip surface on which a co-activator peptide (SRC-1) was immobilized. Ligand-induced association of the hFXR LBD with the SRC-1 peptide was monitored by a change in resonance units (RUs).

Acknowledgment. H.C., H.H., and J.C. were in part supported by BK21 Program, the Ministry of Education, Science and Technology, Korea. This research was supported by grants from the Marine Biotechnology Program funded by the Ministry of Land, Transport and Maritime Affairs of Korea. The authors thank K. N. Maloney for her help in preparing this Note.

Supporting Information Available: NMR spectra of **1**−**3**, NMR data table of **4**−**6**, chromatograms illustrating the separation of **2/3** by enantioselective HPLC, proposed synthetic mechanism of **2** and **3** from **4**, and the effects of **2**−**6** on steroid receptor transactivation. These materials are available free of charge via the Internet at http://pubs.acs.org.

References and Notes

(1) (a) Makishima, M.; Okamoto, A. Y.; Repa, J. J.; Tu, H.; Learned, R. M.; Luk, A.; Hull, M. V.; Lustig, K. D.; Mangelsdorf, D. J.; Shan, B. *Science* **1999**, *284*, 1362–1365. (b) Parks, D. J.; Blanchard, S. G.; Bledsoe, R. K.; Chandra, G.; Consler, T. G.; Kliewer, S. A.; Stimmel, J. B.; Willson, T. M.; Zavacki, A. M.; Moore, D. D.; Lehmann, J. M. *Science* **1999**, *284*, 1365–1368.

(2) Russell, D. W. *Annu. Rev. Biochem.* **2003**, *72*, 137–174.

(3) (a) Rizzo, G.; Renqa, B.; Mencarelli, A.; Pellicciari, R.; Fiorucci, S. *Curr. Drug Targets* **2005**, *5*, 289–303. (b) Fiorucci, S.; Rizzo, G.; Donini, A.; Distrutti, E.; Santucci, L. *Trends Mol. Med.* **2007**, *13*, 298–309. (c) Modica, S.; Moschetta, A. *FEBS Lett.* **2006**, *580*, 5492–5499.

(4) Hartman, H. B.; Gardell, S. J.; Petucci, C. J.; Wang, S.; Krueger, J. A.; Evans, M. J. *J. Lipid Res.* **2009**, *50*, 1090–1100.

(5) Lambert, G.; Amar, M. J.; Guo, G.; Brewer, H. B., Jr.; Gonzalez, F. J.; Sinalll, C. J. *J. Biol. Chem.* **2003**, *278*, 2563–2570.

(6) Zhang, Y.; Wang, X.; Vales, C.; Lee, F. Y.; Lee, H.; Lusis, A. J.; Edwards, P. A. *Arterioscl. Throm. Vas.* **2006**, *26*, 2316–2321.

(7) Guo, G. L.; Santamarina-Fojo, S.; Akiyama, T. E.; Amar, M.; Paigen, B. J.; Brewer, H. B., Jr.; Gonzalez, F. J. *Biochim. Biophys. Acta* **2006**, *1761*, 1401–1409.

(8) (a) Urizar, N. L.; Liverman, A. B.; Dodds, D. T.; Silva, F. V.; Ordentlich, P.; Yan, Y.; Gonzalez, F. J.; Heyman, R. A.; Mangelsdorf, D. J.; Moore, D. D. *Science* **2002**, *296*, 1703–1706. (b) Burris, T. P.; Montrose, C.; Houck, K. A.; Osborne, H. E.; Bocchinfuso, W. P.; Yaden, B. C.; Cheng, C. C.; Zink, R. W.; Barr, R. J.; Hepler, C. D.; Krishnan, V.; Bullock, H. A.; Burris, L. L.; Galvin, R. J.; Bramlett, K.; Stayrook, K. R. *Mol. Pharmacol.* **2005**, *67*, 948–954.

(9) (a) Yu, J.; Lo, J.-L.; Huang, L.; Zhao, A.; Metzger, E.; Adams, A.; Meinke, P. T.; Wright, S. D.; Cui, J. *J. Biol. Chem.* **2002**, *277*, 31441–31447. (b) Nishimaki-Mogami, T.; Une, M.; Fujino, T.; Sato, Y.; Tamehiro, N.; Kawahara, Y.; Shudo, K.; Inoue, K. *J. Lipid. Res.* **2004**, *45*, 1538–1545. (c) Carter, B. A.; Taylor, O. A.; Prendergast, D. R.; Zimmerman, T. L.; von Furstenberg, R.; Moore, D. D.; Karpen, S. *J. Pediatr. Res.* **2007**, *62*, 301–306.

(10) (a) Nam, S.-J.; Ko, H.; Shin, M.; Ham, J.; Chin, J.; Kim, Y.; Kim, H.; Shin, K.; Choi, H.; Kang, H. *Bioorg. Med. Chem. Lett.* **2006**, *16*,

5398–5402. (b) Kainuma, M.; Makishima, M.; Hashimotoa, Y.; Miyachia, H. *Bioorg. Med. Chem.* **2007**, *15*, 2587–2600.
(11) (a) Segawa, M.; Shirahama, H. *Chem. Lett.* **1987**, *16*, 1365–1366. (b) Kusumi, T.; Shibata, Y.; Ishitsuka, M.; Kinoshita, T.; Kakisawa, H. *Chem. Lett.* **1979**, *8*, 277–278.
(12) (a) Gawronski, J. K.; van Oeveren, A.; van der Deen, H.; Leung, C. W.; Feringa, B. L. *J. Org. Chem.* **1996**, *61*, 1513–1515. (b) Braun, M.; Rahematpura, J.; Bühne, C.; Paulitz, T. C. *Synlett* **2000**, *7*, 1070–1072.
(13) Lightner, D. A.; Gurst, J. E. *Organic Conformational Analysis and Stereochemistry from Circular Dichroism Spectroscopy*; John Wiley & Sons: New York, 2000; *Chapter 14*, pp 423−456.
(14) Muckensturm, B.; Diyani, F.; Reduron, J.-P.; Hildenbrand, M. *Phytochemistry* **1997**, *45*, 549–550.
(15) Forman, B. M.; Goode, E.; Chen, J.; Oro, A. E.; Bradley, D. J.; Perlmann, T.; Noonan, D. J.; Burka, L. T.; McMorris, T.; Lamph, W. W.; Evans, R. M.; Weinberger, C. *Cell* **1995**, *81*, 687–693.
(16) Fujino, T.; Sato, Y.; Une, M.; Kanayasu-Toyoda, T.; Yamaguchi, T.; Shudo, K.; Inoue, K.; Nishimaki-Mogami, T. *J. Steroid Biochem. Mol. Biol.* **2003**, *87*, 247–252.

NP100489U